

DFT Calculations for Electron Transfer Bond-breaking Reaction of CH₃-X

Yu Mei XING², Zheng Yu ZHOU^{1,3*}, Ben Ni DU¹

¹Department of Chemistry, Qufu Normal University, Shandong Qufu 273165

²Department of Chemistry, Nankai University, Tianjin 300071

³State Key Laboratory of Crystal Materials, Shandong University, Shandong, Jinan 250100

Abstract: DFT/6-311+g** level calculations are performed to study the electron transfer bond-breaking reaction of CH₃-X. The calculated values are in good agreement with the experimental results or the empirical model. Through analyzing the change of the energy and the charge density along the reaction path, the bond-breaking in ET reaction for CH₃X is investigated.

Keywords: Electron transfer, bond-breaking reaction, density functional theory (DFT), CH₃X.

Bond-breaking in electron transfer (ET) reaction is a powerful synthetic tool to provide alkyl radicals. The reaction $RX + e^- \rightarrow R^\bullet + X^-$ in gas-phase yields directly the alkyl radical and the halide ion. Although *ab initio* calculation has been performed to this kind of reaction for CH₃-X¹⁻³, density functional theory (DFT) has not been invoked so far. DFT is gaining popularity recently as a cost-effective procedure for studying physical properties of molecules.

The activation energy (ΔG^\ddagger) of this type of reaction is obtained from eq (1):

$$\Delta G^\ddagger = \Delta G_0^\ddagger \left(1 + \frac{\Delta G^0}{4\Delta G_0^\ddagger}\right)^2 \quad (1)$$

In the gas phase, the intrinsic barrier (ΔG_0^\ddagger) merely includes the internal reorganization factor, which is one-fourth of the bond dissociation energy (D_{RX}).

The potential energy curve of CH₃-X bond is obtained by Morse type potential. The quadratic force constant (f), the activation parameter (α) and the cubic force constant (g) can be obtained from

$$f = 4\pi^2 c^2 \omega^2 M_X / N_A \quad (2)$$

$$\alpha = \left(\frac{fN_A}{2D_{RX}}\right)^{1/2}, \quad g = 3f^{2/3} \left(\frac{N_A}{2D_{RX}}\right)^{1/2} \quad (3)$$

All calculations were performed using the GAUSSIAN 94 program package. *Ab*

initio and DFT methods were both applied. The 6-311+g** and Lan12dz basis sets are selected.

Results and Discussion

The calculated values are presented in **Table 1**. Compared with *ab initio* method and other theories, the results obtained from B3LYP are much closer to the experimental values. The structures optimized for CH₃X (F, Cl, Br, I) by using B3LYP are illustrated in **Figure 1**.

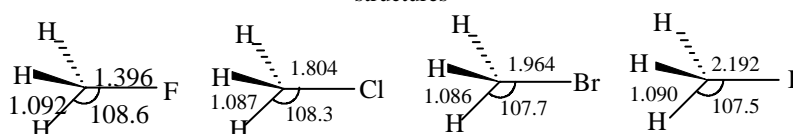
Table 1 The results calculated by using *ab initio* and DFT methods for CH₃X neutral molecules and compared with other theories ($\Delta G^0 = D_{RX} - EA(X)$), EA is the electron affinity of halide

method	R _(C-X) (Å)	ω_{C-X} (cm ⁻¹)	f (mdyn/Å)	α (1/Å)	g (mdyn/Å ²)	D _{RX} (kJ/mol)	EA(X) (kJ/mol)	ΔG^0 (kJ/mol)	
X=F	HF	1.366	1155.4	14.95	3.89	174.20	297.0	131.3	165.6
	MP2	1.389	1076.5	12.98	2.89	112.46	467.3	311.7	155.6
	MP3	1.379	1115.5	13.93	3.10	129.38	453.9	341.4	95.6
	B3LYP	1.396	1033.7	11.96	2.80	100.46	459.4	338.0	121.3
	B3P86	1.385	1066.8	12.74	3.02	115.26	420.0	367.3	52.7
	B3PW91	1.387	1061.5	12.62	2.87	108.78	461.9	324.6	137.2
	Theor ¹	1.40	—	—	—	—	435.5	261.0	174.4
	Theor ⁵	1.391	—	—	—	—	451.8	—	—
	exp.	1.383 ^{6a}	1048.2 ^{4b}	12.30	2.86	105.53	456.9 ^{4c}	333.0 ^{4d}	123.8
X=Cl	HF	1.789	772.9	12.48	3.94	147.86	242.6	262.7	-2 0.0
	MP2	1.776	785.6	12.89	3.33	128.51	249.3	310.0	39.3
	MP3	1.780	781.0	12.74	3.39	129.74	334.3	299.1	35.1
	B3LYP	1.804	728.4	11.08	3.12	103.71	341.4	349.3	-7.9
	B3P86	1.789	739.0	11.40	3.09	105.63	359.4	—	—
	B3PW91	1.790	736.8	11.34	3.12	106.2	351.0	355.6	-4.60
	Theor ¹	1.79	—	—	—	—	330.1	304.1	25.6
	Theor ³	1.82	—	—	—	—	288.2	211.7	76.5
	Theor ⁵	1.788	—	—	—	—	340.5	—	—
exp.	1.781 ^{4e}	732.1 ^{4b}	11.20	3.11	104.69	349.4 ^{4f}	348.1 ^{4d}	12.5	
X=Br	HF	1.945	640.8	19.33	5.42	313.90	197.9	251.0	-53.1
	B3LYP	1.964	593.8	16.60	4.11	205.16	296.6	333.4	-36.8
	B3P86	1.944	615.0	17.81	4.03	214.97	329.6	392.4	-64.8
	B3PW91	1.948	612.1	17.64	4.16	220.25	307.1	342.6	-35.5
	theor ⁵	1.940	—	—	—	—	291.6	—	—
	exp.	1.931 ^{4g}	611.0 ^{4b}	17.58	4.22	222.08	292.8 ^{4h}	324.6 ^{4d}	-28.0
X=I	HF	2.181	529.2	20.94	7.39	464.27	115.4	203.3	-87.8
	MP2	2.194	522.3	20.40	5.28	323.33	220.4	221.7	-1.2
	MP3	2.199	514.8	19.82	5.40	320.94	204.5	217.5	-1 2.9
	B3LYP	2.194	531.2	21.10	5.18	327.32	236.3	294.1	-5 7.7
	B3P86	2.178	520.1	20.23	5.08	308.72	236.3	338.4	-102.0
	B3PW91	2.179	519.1	20.15	5.41	327.34	207.5	296.6	-89.1
	exp.	2.140 ^{4g}	532.8 ^{4b}	21.23	5.21	331.86	235.5 ^{4c}	295.4 ^{4d}	-59.8

It is obvious from **Table 1** that the larger X is, the longer r_{C-X} is, and the smaller the dissociation energy (D_{RX}) is. From the equilibrium state to the infinite dissociation state, the change of hybridization of C atom from sp³ to sp² is involved accompanying with the change of the energy of CH₃-X. Before ET takes place the neutral molecule is more

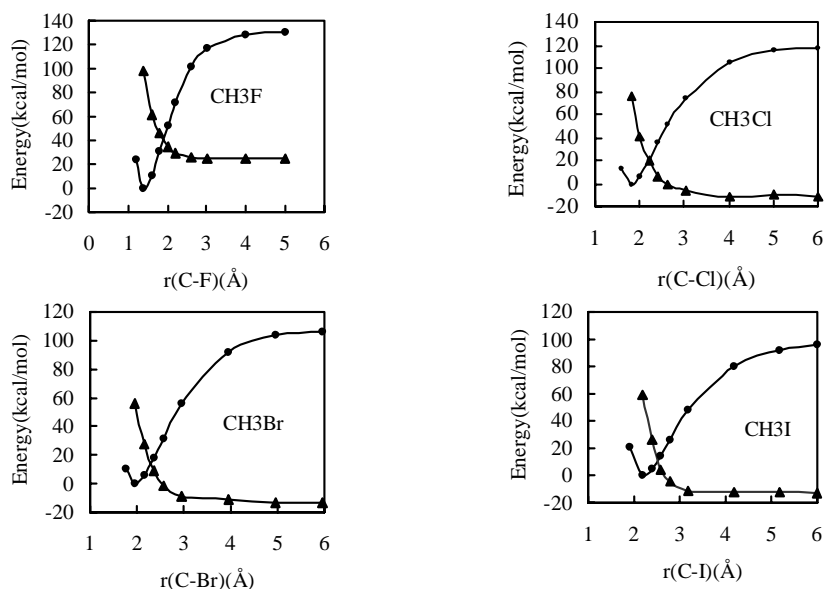
stable than its corresponding anion radical. When the reaction has occurred, the C-X bond is progressively broken and is accompanied by the increasing of the energy of neutral molecule and by the decreasing of the energy of anion radical. These can be seen from **Figure 2**.

Figure 1 B3LYP/6-311+G** (for F, Cl, Br) and B3LYP/LANL2DZ(for I) optimized structures



The cross point of two potential energy curves between CH₃X and CH₃[•] + X⁻ is defined as the transition state. For the neutral molecule, a free electron that does not contribute to the total energy of the system is assumed. The potential energy curve is depicted in **Figure 2**. According to it, the activation characters are listed in **Table 2**. It can be found that the results computed by the B3LYP are in better agreement with those obtained from the empirical model.

Figure 2 The potential energy curves of CH₃X(●) and of CH₃[•] + X⁻(▲)calculated by using B3LYP



The potential curves for the radical anions are generally pretty flat from R[#] to infinite distance. It reflects that the higher negative charge localizes on X⁻. The charge density of X calculated by using B3LYP is listed in **Table 3**. It can be seen that the charge on X atom increases with the enlarging of the C-X bond distance. At the crossing point, the charge on X atom is equal to X⁻, the bond breaking and ET reaction

will take place. The charge increment $\Delta Z(X)$ increases along with the sequence from F, Cl, and Br to I. For F atom, it already possesses a large electronic charge on the neutral structure at the crossing point, so that it is difficult to accept another electron. Moreover, the negative charge of F atom at the transition state (-0.632) is closer to the infinite dissociation state than that of Cl atom. For Cl atom, the negative charge at the transition state (-0.377) is closer to that of the reactant state (-0.169). It means that breaking of C-F bond is faster than that of C-Cl bond at the transition state.

Table 2 The activation characteristics of bond-breaking reaction in gas phase

X	ΔG^\ddagger (kJ/mol) ^a			r^\ddagger (Å)	Δr^\ddagger (Å) ^b
	B3LYP calculations	empirical model			
		C	D		
F	172.7	183.6	180.7	1.90	0.50
Cl	85.30	81.50	87.80	2.20	0.40
Br	59.40	56.90	58.10	2.33	0.36
I	38.00	33.80	32.60	2.51	0.31

^a in the empirical model ΔG^\ddagger is calculated from Eq. (1).

^b $\Delta r^\ddagger = r^\ddagger - r_e$, r_e and r^\ddagger represent the C-X bond length in equilibrium and in transition state, respectively.

^{c,d} D_{RX} and ΔG^0 are obtained by using the B3LYP method or from the experimental values.

Table 3 Negative charge on halogen atom (atomic units)

X	reactant	crossing point		product
	CH ₃ X	CH ₃ X	CH ₃ X ^{•-}	CH ₃ +X ⁻
F	0.483	0.632	0.821	1.000
Cl	0.169	0.377	0.790	1.000
Br	0.097	0.262	0.746	1.000
I	0.046	0.173	0.725	1.000

References

1. M. Hotokka, B. O. Roos, L. Ebersson, *J. Am. Chem. Soc. (Perkin Trans)*, 2nd ed., **1986**, 1979.
2. B. T. Luke, G. H. Loew, A. D. Mclean, *J. Am. Chem. Soc.*, **1987**, 109, 1307; **1988**, 110, 3396.
3. R. Benassi, F. Bernardi, A. Bottoni, M. A. Robb, F. Taddei, *Chem. Phys. Lett.*, **1989**, 161, 79.
4. (a) W. W. Clark, F. C. Delucia, *J. Mol. Struct.*, **1976**, 32, 29. (b) G. Herzberg, *Infrared and Raman Spectra*, Van Nostrand, New York, **1945**, 314. (c) M. W. Chase, NIST-JANAF Thermochemical Table, 4th ed. *J. Phys. Chem. Ref. Data, Monogr*, 9, **1998**, 1-1951. (d) R. S. Berry, S. A. Rice, J. Ross, *J. Physical Chemistry*, Wiley, New York, **1980**. (e) E. Hirota, T. J. Tanaka, *J. Mol. Spectrosc.*, **1970**, 34, 222. (f) M. Weissman, S. W. Benson, *J. Phys. Chem.*, **1983**, 87, 243. (g) S. A. Kudchker, A. P. Kudchaker, *J. Phys. Chem. Ref. Data*, **1975**, 4, 4576. (h) E. T. Roux, S. Paddison, *Int. J. Chem. Kinet.*, **1987**, 19, 15.
5. W. S. Mcgovern, A. D. Kovacs, S. W. North, *J. Phys. Chem. A*, **2000**, 104, 436.

Received 25 September, 2000